Phase transition in diffusion-limited aggregation with two immiscible components

Takashi Nagatani
College of Engineering, Shizuoka University, Hamamatsu 432, Japan

Francesc Sagués
Departament de Quimica-Fisica, Universite de Barcelona, Diagonal 647, E-08028 Barcelona, Spain
(Received 11 April 1991)

A diffusion-limited-aggregation (DLA) model with two immiscible components (A and B atoms) is presented to investigate a phase transition in morphological changes. A segregation occurs where the DLA pattern is constructed by a mixture of trees consisting of only A atoms and trees consisting of only B atoms. Above a critical concentration p_c, trees with only A atoms exceed trees with only B atoms, and the DLA with only A atoms dominates. It is found that a phase transiton between A-DLA and B-DLA occurs at the critical concentration p_c, where A-DLA and B-DLA represent, respectively, DLA with only A atoms and DLA with only B atoms. The phase transition is analyzed by making use of the real-space renormalization-group method. The correlation length ξ scales as $\xi \approx (p-p_c)^{-\nu}$, where $p_c=0.5$ and $\nu=1.85$ on the square lattice.

PACS number(s): 68.70.+w, 05.70.Jk, 05.40.+j

I. INTRODUCTION

Recently there has been increasing interest in a variety of nonequilibrium aggregation and deposition models [1–11]. Fractal growth phenomena in pattern formation have attracted considerable attention. The simplest growth models are ballistic deposition and diffusion-limited aggregation (DLA). The ballistic-deposition model provides a basis for understanding deposition processes used to prepare a wide variety of thin-film devices. The DLA model presents a prototype of the pattern formation of diffusive systems including the electrochemical deposition, crystal growth, viscous fingering, dielectric breakdown, chemical dissolution, and bacterial colonies [12]. A variety of computer simulations have been carried out to investigate the relationships between the cluster geometry and growth mechanisms. The structure of the aggregates strongly depends on the dynamics of the growth process. The crossover phenomena and the geometrical phase transition between the DLA fractal and the nonfractals have been found by computational and experimental methods. The crossover and the phase transition have been analyzed by the real-space renormalization-group method [13–16]. Lee, Coniglio, and Stanley [13] succeeded in analyzing the crossover from the DLA fractal to the dense structure in viscous fingering at the finite viscosity ratio by using the two-parameter position-space renormalization-group method. Nagatani [14] analyzed the effect of the sticking probability on the fractal nature of the DLA. Furthermore, the combined effect of the sticking probability and the finite viscosity ratio was analyzed by using the three-parameter position-space renormalization method [15]. The real-space renormalization-group method will be a powerful tool in analyzing the morphological changes.

Until now, a variety of studies have been done for the pattern formation in the DLA only with a single component [1–24]. However, few investigations for the DLA with two components have been done. There is an open question about whether or not the morphological change occurs. It will be interesting to study the morphological changes in the DLA with two components.

In this paper, we investigate the morphological change in the DLA with two immiscible components (A and B atoms) by using a computer simulation and a real-space renormalization-group method. We restrict ourselves to the limiting case where a connection between A and B atoms is inhibited. An A atom sticks only on the surface consisting of A atoms and a B atom sticks only on the surface consisting of B atoms. In the limiting case, a segregation occurs where the DLA pattern is constructed by a mixture of the trees consisting of only A atoms and the trees consisting of only B atoms. We define the concentration of A atoms as p. One expects that a morphological phase transition occurs between the DLA with only A atoms and the DLA with only B atoms at a critical concentration. We carry out the computer simulation and find the phase transition. We analyze the phase transition by using the real-space renormalization-group method. We give the evidence of the phase transition.

The organization of the paper is as follows. In Sec. II we present the model and the simulation result. In Sec. III we analyze the phase transition by using a small-cell renormalization method. In Sec. IV we derive the critical concentration p_c and the scaling exponent ν of the correlation length by using a Monte Carlo renormalization method. In Sec. V we present the summary.

II. MODEL AND SIMULATION

We consider the DLA with two components (A and B species). We present the two-component DLA model. A and B species diffuse independently. The concentrations

C_A and C_B of the diffusion components satisfy, respectively, the Laplace equations under the quasistationary approximation

$$\nabla^2 C_A = 0, \tag{1a}$$

$$\nabla^2 C_B = 0. \tag{1b}$$

We consider the deposition process on the plate. At the position far from the plate, the concentrations C_A and C_B are, respectively, constants. We consider the boundary condition on the surface of deposit. We define the sticking probabilities P_{AA}, P_{BB}, P_{AB}, and P_{BA}. P_{AA} (P_{BB}) indicates the sticking probability at which an A (B) atom sticks on the surface of A (B) atoms when an A (B) atom lands on the surface of A (B) atoms. P_{AB} (P_{BA}) indicates the sticking probability at which an A (B) atom sticks on the surface of B (A) atoms when an A (B) atom lands on the surface of B (A) atoms. We restrict ourselves to the limiting case $P_{AA}=1$, $P_{BB}=1$, $P_{AB}=0$, and $P_{BA}=0$. Atoms can stick only on the surface consisting of the same atoms. Different atoms cannot stick to each other. Then the boundary conditions are given by

$$(1-P)\frac{\partial C_A}{\partial n} - PC_A = 0, \tag{2a}$$

where

$$P = P_{AA}(=1)$$

if an A atom lands on an A surface and

$$P = P_{AB}(=0)$$

if an A atom lands on a B surface.

$$(1-P)\frac{\partial C_B}{\partial n} - PC_B = 0\ , \tag{2b}$$

where

$$P = P_{BB}(=1)$$

if a B atom lands on a B surface, and

$$P = P_{BA}(=0)$$

if a B atom lands on an A surface. Here, $\partial C/\partial n$ is the derivative normal to the interface.

Now we consider the simulation of the aggregation process following Eq. (1) with the boundary condition (2). The diffusing particles can be simulated by using the random walker. The probability that the random walker visits the site satisfies the discrete version of the Laplace equation. The boundary condition (2) can be simulated by introducing the sticking probability into the random walker. When a particle reaches the surface of the deposit consisting of the same particles, it sticks on the deposit with the probability 1. Otherwise, the particle is reflected on the deposit with the probability 1. We summarize the algorithm of the simulation process. The simulation of the two-component Laplacian growth with the boundary condition (2) is carried out with the use of a simple square lattice. We consider a subset of the square lattice enclosed by a square with 200×200 (units). We start out with an occupied plate on the bottom of the square. The lateral boundary is periodic. An A or B particle is introduced one at a time at a randomly chosen point on the upper boundary. An A particle is introduced with the probability $p=C_A/(C_A+C_B)$ and a B particle with the probability $1-p$. Each particle performs a Brownian motion. The particle continues to move until it either reaches a point adjacent to a site already occupied by a particle or until it reaches the upper boundary. When the particle reaches a point adjacent to a site already occupied by a particle and if the already occupied site is the same kind of particles, it sticks on the aggregate with probability 1. Otherwise, the particle is reflected at the aggregate with probability 1 and continues to move. When the particle reaches the upper boundary, the random walker is annihilated. We repeat the above procedure. The deposits are grown until the height reaches 150 units. Figures 1(a)–1(e) show, respectively, the results for $p=0.1$, 0.3, 0.5, 0.7, and 0.9, obtained by using the procedures outlined above. A segregation occurs where the DLA pattern is constructed by a mixture of the trees consisting of only A atoms and the trees consisting of only B atoms. The upper, middle, and bottom patterns in each figure indicate, respectively, the deposits consisting of $A+B$ atoms, the trees of A atoms within the deposit, and the trees of B atoms within the deposit. For $p=0.1$ and 0.3, the trees of B atoms exceed the trees of A atoms. The tree of B atoms spans from the plate to the top. The tree of B atoms dominates at larger length scales than the characteristic length until both the A and B trees coexist. On the other hand, for $p=0.7$ and 0.9, the trees of A atoms exceed the trees of B atoms. The tree of A atoms spans from the plate to the top. The tree of A atoms dominates at larger length scales than the characteristic length until both the A and B trees coexist. At $p=0.5$, both the A and B trees span from the plate to the top. The characteristic length, until which both the A and B trees coexist, ranges over all the space. In the limit of $p=0$, the DLA fractal with only B atoms is reproduced. In the limit $p=1$, the DLA fractal with only A atoms is reproduced. One expects that a phase transition occurs between the A-DLA and the B-DLA at the critical concentration $p\approx0.5$, where A-DLA and B-DLA represent the DLA with only A atoms and DLA with only B atoms, respectively.

We apply the real-space renormalization-group method to this problem in the following sections to give evidence of the phase transition.

III. SMALL-CELL RENORMALIZATION

We analyze the phase transition by making use of the real-space renormalization-group method. For simplicity, we apply the small-cell renormalization first. In Sec. IV, we shall consider the large-cell renormalization. We assume that at the critical concentration p_c a mixture of A and B trees is self-similarly distributed. Above or below the critical concentration, the deposit crosses over from the self-similar mixture to the A-DLA or B-DLA at

the characteristic length ξ. We define the characteristic length as the correlation length. We perform the renormalization in a similar way to the percolation [25]. Here we consider the bond model. The A and B species occupy the bonds on the lattice. The deposit is constructed from the occupied A and B bonds. We replace a cell of bonds by a single superbond. We define the superbond representing the cell of length b (scale factor) as an A bond if the cell contains a spanning cluster connecting opposite lines by A bonds. The superbond is defined as a B bond if the cell contains a spanning cluster connecting opposite lines by B bonds. We renormalize the concentration p in a similar way to the bond percolation. Only right at the critical point, where self-similarity of the mixture is valid, do we have $p'=p=p_c$. The correlation length ξ limits the validity of similarity of the mixture; thus this limit ξ is the same in both the original lattice and the renormalized lattice of superbonds, $\xi=\xi'$. If in

FIG. 1. Typical patterns with two immiscible components (A and B species) grown by varying the concentration p of A species. The upper, middle, and bottom patterns in each figure indicate, respectively, the deposits consisting of $A+B$ species, the trees of A species within the deposit, and the trees of B species within the deposit. (a) $p=0.1$, (b) $p=0.3$, (c) $p=0.5$, (d) $p=0.7$, (e) $p=0.9$.

the original lattice we have $\xi=\text{const}|p-p_c|^{-\nu}$, then in the renormalized lattice, with lattice constant b, we have $\xi'=\text{const}b|p'-p_c|^{-\nu}$, with the same proportionality constant and the same critical exponent ν:

$$b|p'-p_c|^{-\nu}=|p-p_c|^{-\nu} . \tag{3}$$

This is the basic equation of real-space renormalization. Taking the logarithm of both sides we arrive at

$$1/\nu=\ln[(p'-p_c)/(p-p_c)]/\ln(b) \tag{4}$$

for the exponent of the correlation length.

We consider the renormalization procedure for deriving the renormalization-group equation for the concentration: $p'=R(p)$. We partition all the space of the square lattice into cells of size $b=2$ (b is the scale factor). After a renormalization transformation these cells play the role of "renormalized" bonds. The renormalized bonds are then classified into the two types of bonds. If the cell is spanned with the occupied A bonds, the renormalized bond is then considered to be the A bond. If the cell is spanned with the occupied B bonds, then the cell is renormalized as the B bond. After renormalization, the concentration p is transformed to p'. For the square lat-

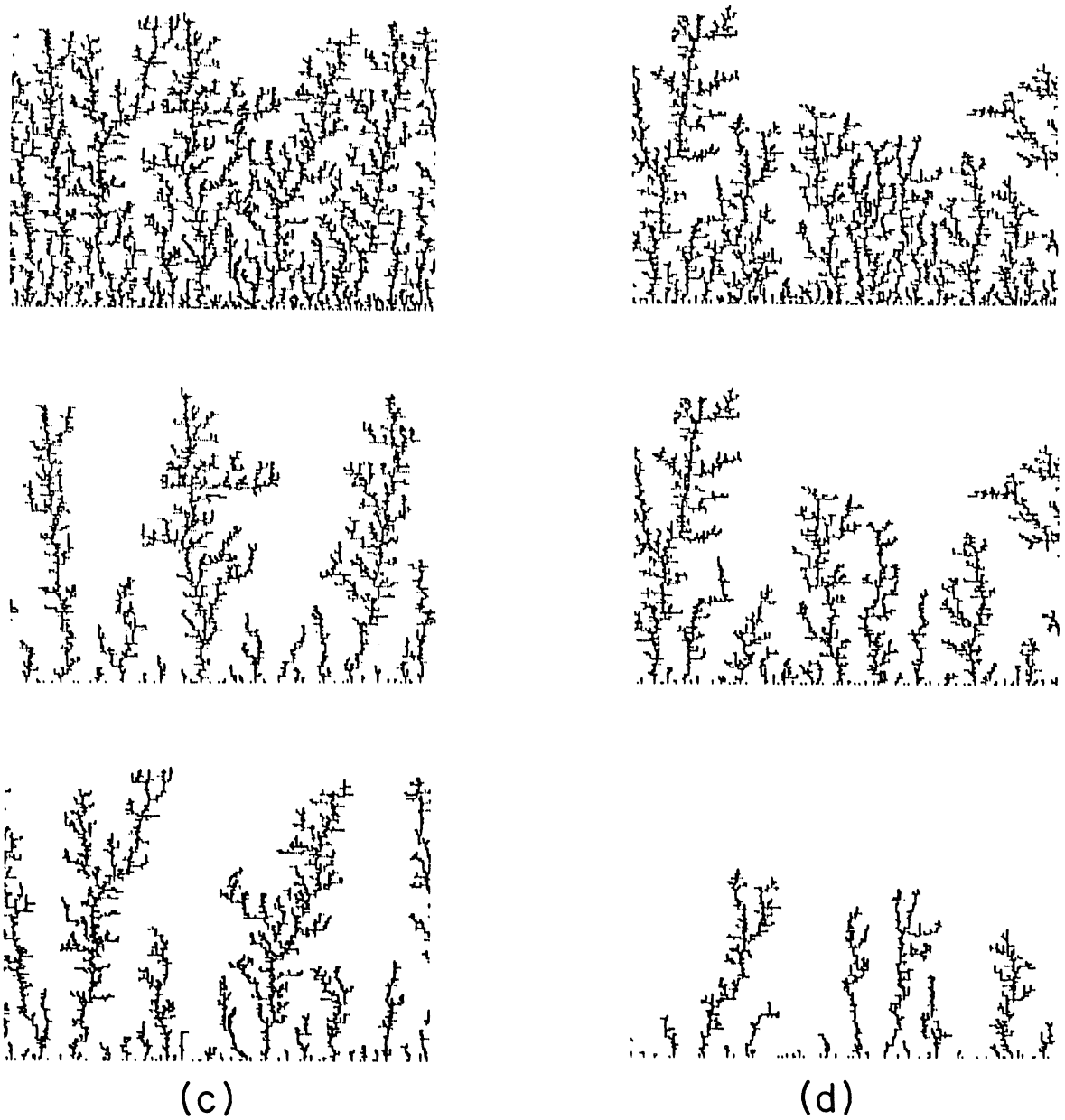

FIG. 1. (*Continued*).

tice, Fig. 2 shows all the configurations of the cell for which it is possible to renormalize as the A bond. The bonds occupied by A species are indicated by the bold lines. The bonds occupied by B species are represented by the dotted lines. Let us consider the configurational probability C_α with which a particular configuration α appears. The distinct configurations are labeled by α ($\alpha=a,b,c,d$) in Fig. 2. The configurational probabilities C_α can be calculated by considering the growth process within the cell. The growth process within the cell is shown in Fig. 3. The configurations (a) or (b) in Fig. 3 are constructed by adding A or B species on the lower bonds.

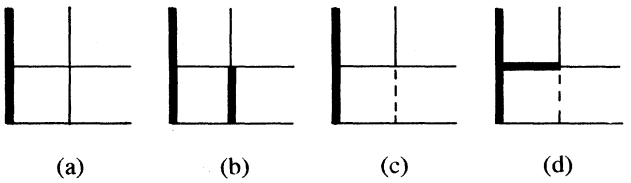

FIG. 2. All the configurations of the cell for which it is possible to renormalize as the A bond for $b=2$. The distinct configurations are labeled by α ($\alpha=a,b,c,d$). The bonds occupied by A species and B species are indicated by the bold and dotted lines, respectively.

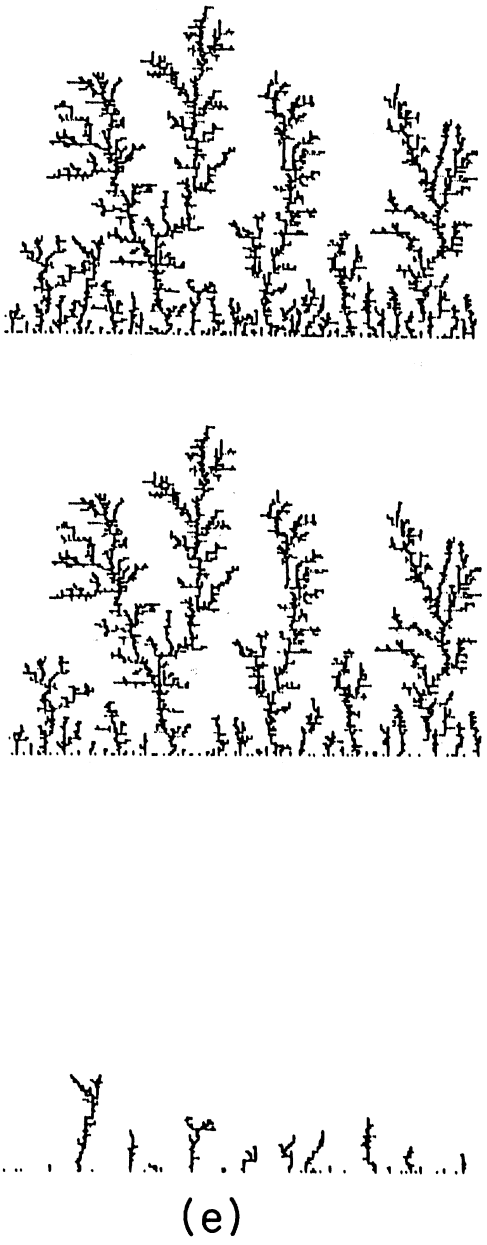

FIG. 1. (*Continued*).

The configurational probabilities C_a and C_b are given by

$$C_a=p \quad \text{and} \quad C_b=1-p. \tag{5}$$

The configurations (c) and (d) in Fig. 3 are constructed by adding A species on the configuration (a). The configurational probabilities C_c and C_d are given by

$$C_c=p^2p_1 \quad \text{and} \quad C_d=3p^2p_2, \tag{6}$$

where p_1 and p_2 are the growth probabilities of the bonds within the configuration (a). The growth probability of the bond is proportional to the current or electric field on the bond. The constant voltage is applied between the

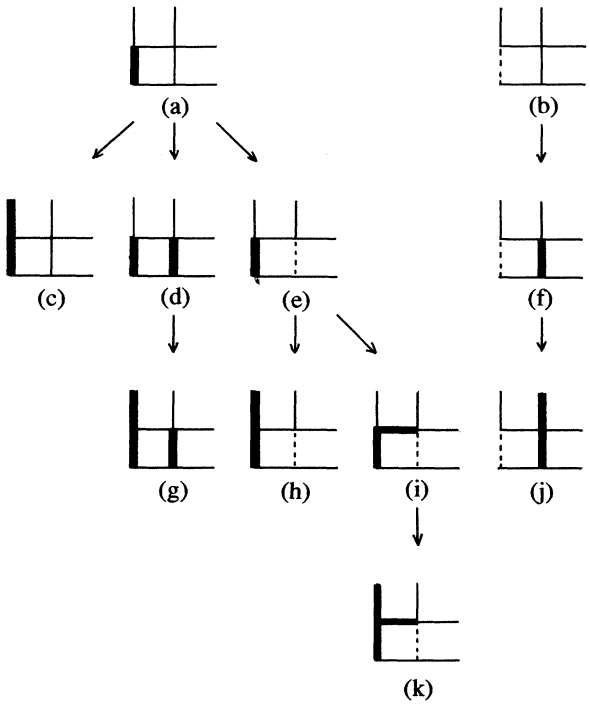

FIG. 3. The growth process within the cell for $b=2$. The configurational probability C_α for the distinct configurations can be calculated by considering the growth process. The bonds occupied by A and B species are represented by the bold and dotted lines, respectively.

top and the bottom within the cell. The lateral boundary condition is periodic in the cell. The growth probabilities p_1 and p_2 are given by

$$p_1=\frac{4}{7} \quad \text{and} \quad p_2=\frac{1}{7}. \tag{7}$$

The configuration (e) is constructed by adding B species on the configuration (a). The configurational probability C_e is given by

$$C_e=p(1-p). \tag{8}$$

Similarly, we can obtain the configurational probabilities C_f, C_g, C_h, C_i, C_j, and C_k:

$$\begin{aligned} C_f&=(1-p)p, \\ C_g&=3p^3p_2, \\ C_h&=p^2(1-p)p_a, \\ C_i&=2p^2(1-p)p_b, \\ C_j&=(1-p)p^2, \\ C_k&=2p^3(1-p)p_b, \end{aligned} \tag{9}$$

where p_a and p_b are the growth probabilities of the bonds in the configuration (e) and are given by

$$p_a=\frac{3}{5} \quad \text{and} \quad p_b=\frac{1}{5}. \tag{10}$$

The configurations (c), (g), (h), (j), and (k) give the configuration spanned by A species. Thus, we obtain the configurational probabilities of the spanning clusters of A species in Fig. 2. The renormalized concentration p' is given by

$$\begin{aligned} p'&=R(p) \\ &=-2p_bp^4+(3p_2-p_a+2p_b-1)p^3+(p_1+p_a+1)p^2. \end{aligned} \tag{11}$$

Figure 4 shows the renormalization function $p'=R(p)$. The renormalization equation has three fixed points:

$$p^*=0,\ 0.691, \text{ and } 1. \tag{12}$$

The first (zero) and the last (unity) fixed points are stable. The middle (0.691) fixed point is unstable. After many repeated renormalizations, the concentration p sucks into the unity fixed point above the unstable fixed point. Below the unstable fixed point, the concentration p sucks into the zero fixed point. At the unstable fixed point, the phase transition occurs. The fixed point $p^*=0.691$ is identified with the critical point p_c in the phase transition. The real-space renormalization group gives the evidence of the phase transition. The correlation length exponent ν is given by

$$\nu=\ln(2)/\ln\left[\frac{dR(p)}{dp}\right]_{p=p_c}=2.212. \tag{13}$$

The values of p_c and ν are not accurate in the small-cell renormalization. We perform the Monte Carlo renormalization of the larger cell in Sec. IV.

IV. MONTE CARLO RENORMALIZATION

We present a Monte Carlo renormalization method to derive the critical concentration p_c and the correlation length exponent ν more accurately. We restrict ourselves to the DLA problem on the square lattice. We extend the small-cell renormalization method to larger-cell renormalization because small-cell renormalization gives somewhat inaccurate values. In general, it is difficult to renormalize a square cell with numerous bonds analytically. Thus we simulate the spanning cells with A bonds by the well-known Monte Carlo method, and then renormalize them. Similar to the bond percolation, we check whether the large cell percolates with A bonds, that is, whether it is spanned by a cluster connecting the top and bottom. We see that the renormalized cell occupation probability p' of A bonds is nothing but the spanning probability $R(p)$ with A bonds. A cell of the type used here is the same as the simulation model with $b\times b$ square. We make a Monte Carlo realization for the spanning cluster with A or B bonds similarly to the simulation in Sec. II. We count the spanning clusters with A bonds. We calcu-

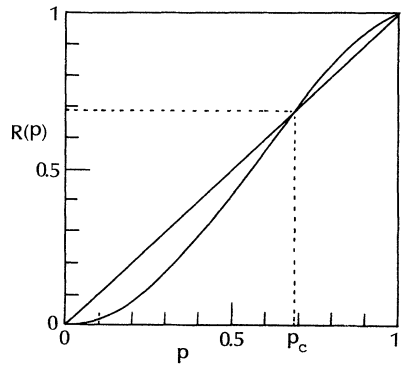

FIG. 4. The renormalization function $p'=R(p)$ obtained from the small-cell renormalization for $b=2$. There is a nontrivial fixed point $p_c=0.691$.

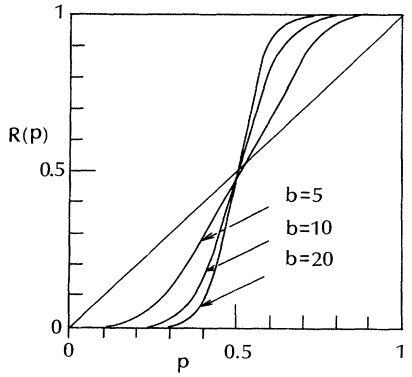

FIG. 5. The renormalization functions $p'=R(p)$ obtained from the Monte Carlo renormalization for $b=5$, 10, and 20.

late the spanning probability $R(p)$ with varying the concentration p. We obtain the spanning probability $R(p)$ from 100 Monte Carlo realizations. Figure 5 shows the spanning probabilities for $b=5$, 10, and 20. The obtained values of the critical concentration p_c and the correlation length exponent ν are given by

$$p_c=0.532\pm0.03 \quad \text{and} \quad \nu=2.32\pm0.4 \quad \text{for } b=5,$$
$$p_c=0.502\pm0.02 \quad \text{and} \quad \nu=1.84\pm0.1 \quad \text{for } b=10, \qquad (14)$$
$$p_c=0.498\pm0.02 \quad \text{and} \quad \nu=1.86\pm0.1 \quad \text{for } b=20.$$

With increasing cell size, the spanning probability $R(p)$ has a trend to approach the step function $\Theta(p-p_c)$, where $p_c=0.5$. Our method converges very rapidly with an increase in the size of the cell. We obtain the critical probability $p_c=0.5$ and the correlation length exponent $\nu=1.85$. By comparing these values with those of the bond percolation on the square lattice, we find that the critical concentration is consistent with the value of the bond percolation and the correlation length exponent is different from the value of the bond percolation. The phase transition between A-DLA and B-DLA belongs to a different universality class with the percolation.

Here we comment on why the small-cell renormalization result $p_c=0.691$ is so different from the values $p_c=0.5$ obtained by the Monte Carlo renormalization. Until now, the small-cell renormalization method has frequently been applied to the percolation problem. The critical probability p_c obtained from the small-cell renormalization strongly depends on the renormalization rules. Especially, the result is dependent upon the type of the cells. In this paper, we used the same type of cells as the bond percolation. In the bond percolation, the critical probability p_c obtained from the cell gives the exact value 0.5. However, in the DLA with two immiscible components, the critical concentration obtained from the same cell does not give an accurate value. This is due to the nonlocal character of the growth probability in the DLA. The bond percolation is determined by the local rule but the DLA is governed by the Laplacian field around the aggregate. The Laplacian field strongly depends on the shape of the aggregate. The growth probability on the perimeter of the aggregate is given by the harmonic measure. The phase transition in the two-component DLA is governed by this nonlocality of the growth probability. For this reason, the small-cell renormalization result does not give an accurate value.

V. SUMMARY

We investigated the diffusion-limited aggregation with two immiscible components (A and B species). We found that a phase transition occurs from the DLA consisting of the B species to the DLA consisting of the A species with an increasing concentration of the A species. We analyzed the phase transition by using the real-space renormalization-group method. We obtained the evidence of the phase transition. We obtained the critical concentration $p_c=0.5$ and the correlation length exponent $\nu=1.85$.

[1] T. A. Witten and L. M. Sander, Phys. Rev. Lett. **47**, 1400 (1981); Phys. Rev. B **27**, 5686 (1983).
[2] P. Meakin, Phys. Rev. A **26**, 1495 (1983); **27**, 2616 (1983).
[3] *Kinetics of Aggregation and Gelation,* edited by F. Family and D. P. Landau (North-Holland, Amsterdam, 1984).
[4] *On Growth and Form,* edited by H. E. Stanley and N. Ostrowsky (Nijhoff, The Hague, 1985).
[5] *Fractals in Physics,* edited by L. Pietronero and E. Tosatti (North-Holland, Amsterdam, 1986).
[6] H. J. Herrmann, Phys. Rep. **136**, 153 (1986).
[7] P. Meakin, in *Phase Transitions and Critical Phenomena,* edited by C. Domb and J. L. Lebowitz (Academic, New York, 1988), Vol. 12, p. 336.
[8] R. Julien and R. Botet, *Aggregation and Fractal Aggregates* (World Scientific, Singapore, 1987).
[9] J. Feder, *Fractals* (Plenum, New York, 1988).
[10] *Random Fluctuations and Pattern Growth,* edited by H. E. Stanley and N. Ostrowsky (Kluwer Academic, Dordrecht, 1988).
[11] T. Vicsek, *Fractal Growth Phenomena* (World Scientific, Singapore, 1989).
[12] H. Fujikawa and M. Matsushita, J. Phys. Soc. Jpn. **58**, 3875 (1989).
[13] J. Lee, A. Coniglio, and H. E. Stanley, Phys. Rev. A **41**, 4589 (1990).
[14] T. Nagatani, Phys. Rev. A **40**, 7286 (1989).
[15] T. Nagatani and H. E. Stanley, Phys. Rev. A **41**, 3263 (1990).
[16] T. Nagatani, J. Lee, and H. E. Stanley, Phys. Rev. Lett. **66**, 616 (1991).
[17] J. D. Sherwood, J. Phys. A **19**, L195 (1986).
[18] M. J. King and H. Scher, Phys. Rev. A **41**, 874 (1990).
[19] G. Daccord and R. Lenormand, Nature (London) **325**, 41 (1987).
[20] M. Murat and A. Aharony, Phys. Rev. Lett. **57**, 1875 (1986).
[21] V. Horvath, J. Kertesz, and T. Vicsek, Europhys. Lett. **4**, 1133 (1987).
[22] R. F. Voss, J. Stat. Phys. **36**, 861 (1984).
[23] D. Grier, E. Ben-Jacob, Roy Clarke, and L. M. Sander, Phys. Rev. Lett. **56**, 1264 (1986).
[24] H. E. Stanley, A. Bunde, S. Havlin, J. Lee, E. Roman, and S. Schwarzer, Physica A **168**, 23 (1990).
[25] D. Stauffer, *Introduction to Percolation Theory* (Taylor & Francis, London, 1985).